Available online at www.sciencedirect.com
ScienceDirect
Metabolism Clinical and Experimental 60 (2011) 805–814
Metabolism
Clinical and Experimental
www.metabolismjournal.com

Regulation of synthesis and oxidation of fatty acids by adiponectin receptors (AdipoR1/R2) and insulin receptor substrate isoforms (IRS-1/-2) of the liver in a nonalcoholic steatohepatitis animal model

Tokio Matsunami, Yukita Sato*, Satomi Ariga, Takuya Sato, Toshiko Shimomura, Haruka Kashimura, Yuki Hasegawa, Masayoshi Yukawa

Laboratory of Biomedical Science, Department of Veterinary Medicine, College of Bioresource Sciences, Nihon University, Fujisawa 252-0880, Japan

Received 15 March 2010; accepted 26 July 2010

Abstract

Nonalcoholic steatohepatitis (NASH) is one of the most frequent causes of abnormal liver dysfunction associated with synthesis and oxidation of fatty acids. Adiponectin receptors (AdipoR1/R2) and insulin receptor substrates (IRS-1/-2) are known as modulators of these fatty acid metabolisms in the liver; however, the regulatory roles of these receptors in the synthesis and oxidation of fatty acids are unclear in the liver of NASH. In this study, we examined the roles of hepatic AdipoR1/R2 and IRS-1/-2 in NASH using an animal model. After feeding a high-fat and high-cholesterol diet to obese *fa/fa* Zucker rats for 8 weeks, rats showed fatty liver spontaneously with inflammation and fibrosis that are characteristic of NASH. The expression levels of AdipoR1/R2 and IRS-2 were significantly decreased, whereas IRS-1 was significantly increased, in NASH. As a result of the decrease of AdipoR1/R2 expression, the messenger RNA expression levels of genes located downstream of AdipoR1/R2, adenosine monophosphate–activated protein kinase α1/α2, which inhibits fatty acid synthesis, and peroxisome proliferator–activated receptor α, which activates fatty acid oxidation, also decreased. Expression level of sterol regulatory element binding protein–1c was found to be elevated, suggesting the up-regulation of IRS-1, and resulted in increased fatty acid synthesis. Furthermore, increase of forkhead box protein A2 expression was observed, which might be associated with the down-regulation of IRS-2, facilitating fatty acid oxidation. Taken together, increased synthesis and oxidation of fatty acids by up- or down-regulation of AdipoR or IRS may contribute to the progression of NASH. Thus, AdipoR and IRS might be crucially important regulators for the synthesis and oxidation of fatty acids in the liver of NASH.

1. Introduction

Obesity, especially visceral fat accumulation, causes insulin resistance, a common risk factor for hepatic steatosis. Fatty liver is thought to represent the first step toward the subsequent development of liver fibrosis. Impaired mitochondrial function provides the second “hit” and promotes the generation of reactive oxygen species (ROS), which promote lipid peroxidation, the release of inflammatory cytokines, death of hepatocytes, and activation of hepatic stellate cells [1]. Nonalcoholic steatohepatitis (NASH) is a progressive disorder that can lead to liver cirrhosis and even hepatocellular carcinoma [2]. Nonalcoholic steatohepatitis is often associated with obesity and/or insulin resistance; however, the precise cause of NASH remains unclear. It is important, therefore, to characterize lipid metabolism, particularly fatty acid metabolism, in NASH.

Adiponectin is a 30-kd hormone produced by adipose tissue that plays an important role in the regulation of whole-body insulin sensitivity [3,4]. The insulin-sensitizing effect of adiponectin appears to be mediated by an increase in fatty acid oxidation, leading to a reduction in the lipid content of liver and skeletal muscle [4,5]. Two types of adiponectin receptors (AdipoR1/R2) clearly differ in their signaling pathways. AdipoR1 is more tightly linked to the activation of the adenosine monophosphate–activated protein kinase (AMPK) pathway and regulates the inhibition of hepatic glucose production together with

* Corresponding author. Tel.: +81 466 84 3445; fax: +81 466 84 3445.
E-mail address: sato.yukita@nihon-u.ac.jp (Y. Sato).

0026-0495/$ – see front matter © 2011 Elsevier Inc. All rights reserved.
doi:10.1016/j.metabol.2010.07.032

increased fatty acid oxidation, whereas AdipoR2 is mainly involved in the activation of the peroxisome proliferator–activated receptor α (PPARα) pathway, which stimulates energy dissipation by increasing fatty acid oxidation [6]. Recently, it was reported that adiponectin showed an hepatoprotective action in nonalcoholic fatty liver disease (NAFLD) [7]. Plasma adiponectin level is decreased in patients with steatosis and NASH, correlating with the severity of liver histology [8]. Considering adiponectin receptors, contradictory results have been published, AdipoR1/R2 expressions being reported as either significantly decreased [9] or increased [10] in the liver of NASH. Therefore, the association between adiponectin receptors and NASH remains unclear.

Insulin is a well-known stimulator of lipogenesis and activates the hepatic expression of sterol regulatory element binding protein–1c (SREBP-1c) [11,12]. Insulin receptor substrate (IRS) proteins, a family of docking molecules, transmit insulin receptor activation signals to essential downstream cascades; and the 2 major isoforms, IRS-1/-2, are expressed in the liver [13]. Generally, IRS-2 is linked more closely to lipid metabolism and both IRS-1/-2 are linked to fatty acid oxidation through the inhibition of a transcription factor, forkhead box protein A2 (Foxa2) [14,15]. It is well known that insulin resistance is associated with decreased expression of IRS-1/-2 [16-18], whereas it has been reported that IRS-1 protein levels, but not IRS-2, were slightly increased in the liver of rats fed a high-fat diet [19]. However, the regulatory roles of IRS-1/-2 remain poorly understood in the liver of NASH. Moreover, to our knowledge, there is no study on the modulating roles of synthesis and oxidation of fatty acids by AdipoR1/R2 and IRS-1/-2 in the NASH condition. Therefore, in the present study, we examined the lipid metabolism roles of AdipoR1/R2 and IRS-1/-2 expression in the liver of NASH, using a high-fat and high-cholesterol (HFC) diet–fed obese rats (Zucker fatty). To achieve this aim, we analyzed (1) metabolic parameters, such as blood biochemical, oxidative stress, lipid peroxidation, and histopathology, in an animal model of NASH; (2) adiponectin expression in the epididymal fat depots, and adiponectin receptors (AdipoR1/R2) and insulin receptor substrate (IRS-1/-2) expression in the liver; (3) the expression of genes related to de novo synthesis of fatty acids in AdipoR1/R2 or IRS-1/-2 downstream effectors (AMPKα1/α2, acetyl–coenzyme A [CoA] carboxylase [ACC], fatty acid synthase [FAS], SREBP-1c); and (4) the expression of genes related to fatty acid oxidation in mitochondria, peroxisomes, and microsomes in AdipoR1/R2 or IRS-1/-2 downstream effectors (carnitine palmitoyltransferase [CPT]-1a, PPARα, uncoupling protein [UCP]–2, straight-chain acyl-CoA oxidase [ACOX], cytochrome P-450 [CYP] 2E1/CYP4A1, Foxa2). Furthermore, we investigated the expression of genes related to synthesis of monounsaturated fatty acids from saturated fatty acids (stearoyl-CoA desaturase 1 [SCD1]), and endoplasmic reticulum (ER) stress (activation transcription factor 3 [ATF3], X-box–binding protein–1 [XBP1], CCAAT/enhancer-binding homologous protein [CHOP]).

2. Materials and methods

2.1. Animal study design

Eight-week-old obese *fa/fa* Zucker rats (n = 16 males) were obtained from Japan SLC Inc (Shizuoka, Japan) and fed rat chow for 1 week. All experimental procedures were implemented in accordance with the Institutional Guidelines for Animal Experiments at the College of Bioresource Sciences, Nihon University, under the permission of the Committee of Experimental Animal in our college. All rats were housed in an animal facility with controlled temperature and a 12-hour light/dark cycle (light on at 7:00 AM and off at 7:00 PM) and had unlimited access to water. The rats (n = 16) were allowed to acclimatize for 1 week before treatment and then randomly divided into 2 groups: control diet (the control rats) or HFC diet groups (the HFC rats), and fed with either a control diet or an HFC diet for 8 weeks, respectively. The control diet (3.6 kcal/g) was low in total fat (5% of total calories were from fat provided by soy oil), and most of the fat was linoleic acid (Table 1, 47% linoleic acid). The HFC diet (4.7 kcal/g) contained 50% of total calories as lard and beef tallow and 5% cholesterol, and was enriched in oleic acid and the saturated fatty acids palmitic and stearic acids (Table 1). Both diets were purchased from Oriental Yeast (Tokyo, Japan). Rats fed the control diet had free access to water, and rats fed the HFC diet had free access to a sodium chloride solution (1%) ad libitum at all times. The mean food intake of the animals in all groups was measured 3 times a week and then averaged to calculate daily food intake. Body weight and biochemical indices were monitored once a week for 8 weeks. After 8 weeks of monitoring, the rats were fasted overnight before a blood sampling was performed. Blood samples were collected from the inferior vena cava just before the rats were killed. Blood samples were centrifuged at 3000 rpm for 5 minutes, and then the plasma or serum was collected and stored at −80°C until analysis. Animals in both treatment groups were killed the following day under ether anesthesia, and then liver weight and intraabdominal fat (epididymal fat pad, mesenteric fat, and perinephric fat) weight were measured. In addition, a

Table 1
Fatty acid profile of the source of fat in the control and the HFC diets expressed as a percentage

Fatty acid profile	Control	HFC
Myristic (14:0)	0.4	2
Palmitic (16:0)	14.6	24.7
Palmitoleic (16:1)	0.7	2.5
Stearic (18:0)	2.6	15.6
Oleic (18:1)	24.6	42.9
Linoleic (18:2)	46.6	7.2
Linolenic (18:3)	3.8	0.6

liver sample was collected in liquid nitrogen for analysis of antioxidant defense enzymes, lipid peroxidation, and the hepatic triglyceride content, and stored at −80°C until analysis. Similarly, liver and epididymal fat depots samples were collected in RNAlater solution (Qiagen, Hilden, Germany) for molecular analysis and stored at −80°C until analysis. In addition, liver tissues samples were fixed overnight in 10% buffered formalin for histopathologic analysis.

2.2. Biochemical analysis

Fasting plasma glucose, total cholesterol, triglyceride, and alanine aminotransferase (ALT) concentrations were measured using commercially available enzyme-linked colorimetric diagnostic kits (DRI-CHEM4000, FUJIFLIM, Tokyo, Japan); and serum concentration of nonesterified fatty acids (NEFAs) was measured by an enzyme method using a JCA-BM2250 (JEOL, Tokyo, Japan). Fasting plasma insulin concentration was determined using a Rat Insulin ELISA KIT (AKRIN-010H; Shibayagi, Gunma, Japan).

2.3. Analysis of antioxidant defense enzymes, lipid peroxidation, and the hepatic triglyceride content

Liver homogenates were prepared as a 1:10 (wt/vol) dilution in pH-7.4, 10-mmol/L potassium phosphate buffer using an Ultra-Turrax (IKA Japan, Nara, Japan). Samples were centrifuged at 3000 rpm for 10 minutes at 4°C, and the supernatants were collected and immediately assayed for enzyme activities. For total glutathione (GSH), approximately 50 μg of liver was homogenized in 5% trichloroacetic acid at a ratio of 1:10 (wt/vol) and centrifuged for 5 minutes at 8000 rpm and 4°C. Total GSH was measured in the tissues as previously described [20]. In addition, total superoxide dismutase (SOD), catalase (CAT), and total glutathione peroxidase (GPx) activities were measured according to Sun et al [21], Aebi [22], and Paglia and Valentine [23], respectively. Lipid peroxidation levels were measured by the thiobarbituric acid reaction using the method of Ohkawa et al [24]. For quantification of the hepatic triglyceride content, the liver was lysed with the buffer in a commercially available kit (TG E-test; Wako, Osaka, Japan) and disrupted by sonication. The triglyceride content of the homogenate was then determined with the previously mentioned kit according to the manufacturer's instructions.

2.4. Liver histopathologic examination

Liver tissue samples were fixed overnight in 10% buffered formalin and embedded in paraffin. Sections (5 μm) of liver tissue were stained with hematoxylin and eosin and Mason trichrome. Steatosis, activity (inflammation), and stage (fibrosis) were semiquantitatively evaluated according to the standard criteria of grading and staging for NASH with minor modifications [25]. Degree of steatosis was scored as the percentage of hepatocytes containing lipid droplets. Activity was evaluated as the sum of scores (score 0-6) of acinar inflammation (score 0-3) and portal inflammation (score 0-3). Fibrosis was graded from 0 (absent) to 4 (1, perisinusoidal/pericellular fibrosis; 2, periportal fibrosis; 3, bridging fibrosis; 4, cirrhosis).

2.5. RNA extraction and quantitative real-time polymerase chain reaction

RNA isolation was performed by homogenization with a Micro Smash-100R (TOMY SEIKO, Tokyo, Japan) using Isogen (NIPPON GENE, Tokyo, Japan) for liver and epididymal fat depots. RNA purification was carried out using the RNeasy Mini kit (Qiagen) in all the tissues studied. All samples were treated with DNase I (RNase Free DNase set, Qiagen). The concentrations of total RNA were measured by absorbance at 260 nm using a NanoDrop ND-1000 (NanoDrop Products, Wilmington, DE, USA). The purity was estimated by the 260:280-nm absorbance ratio. One microgram total RNA was subjected to reverse transcription using an oligo(dT)$_{12\text{-}18}$ primer and M-MuLV reverse transcriptase (SuperScript III First-Strand Synthesis; Invitrogen Life Science, Carlsbad, CA, USA) according to the manufacturer's instructions. The transcript levels of specific primers (Table 2) were quantified by real-time polymerase chain reaction (PCR) (7500 Real-Time PCR System, Applied Biosystems, Foster City, CA). The complementary DNA was amplified under the following conditions: 95°C for 10 minutes, followed by 45 cycles of 15 seconds at 95°C and 1 minute at 59°C, using Power SYBR Green PCR Master Mix (Applied Biosystems). The primer concentrations were 400 nmol/L, respectively. After PCR, a melting curve analysis was performed to demonstrate the specificity of the PCR product, which was displayed as a single peak (data not shown). Every sample was analyzed in triplicate. The relative expression ratio (R) of a target gene was expressed for the sample vs the control in comparison to the 18S ribosomal RNA (rRNA) [26]. R was calculated based on the following equation [27]: $R = 2^{-\Delta\Delta Ct}$, where C_t represents the first cycle at which the fluorescence signal was significantly different from the background and $\Delta\Delta C_t$ is $(C_{t,\ \text{target}} - C_{t,\ 18s\ rRNA})_{\text{treatment}} - (C_{t,\ \text{target}} - C_{t,\ 18s\ rRNA})_{\text{control}}$.

2.6. Data analysis

The results are expressed as means ± standard error of mean (SEM). An unpaired t test with a P value of $< .05$ was used to determine statistical significance.

3. Results

3.1. Metabolic parameters

The general metabolic profiles of the animals are summarized in Table 3. The baseline body weight of the rats at the beginning of the study was similar in all groups. The body weight gain and the final weight of all rats fed the

Table 2
Primers sequences used for real-time PCR reactions

Gene	GenBank accession no.	Forward 5′ → 3′	Reverse 5′ → 3′
Adipoq	NM_144744	GGGAGACGCAGGTGTTCTTG	CGCTGAATGCTGAGTGATACATG
AdipoR1	NM_207587	TCATCTACCTCTCCATCGTCTGTGT	CAAGCCAAGTCCCAGGAACA
AdipoR2	NM_001037979	CATGTTTGCCACCCCTCAGTA	ATGCAAGGTAGGGATGATTCCA
IRS-1	NM_012969	TGTGCCAAGCAACAAGAAAG	ACGGTTTCAGAGCAGAGGAA
IRS-2	AF087674	CTACCCACTGAGCCCAAGAG	CCAGGGATGAAGCAGGACTA
AMPKα1	NM_019142	GGGATCCATCAGCAACTATCG	GGGAGGTCACGGATGAGG
AMPKα2	NM_023991	CATTTGTGCAAGGCCCCTAGT	GACTGTTGGTATCTGCCTGTTTCC
SREBP-1c	XM_213329	GCAACACTGGCAGAGATCTACGT	TGGCGGGCACTACTTAGGAA
ACCα	NM_022193	TGAAGGGCTACCTCTAATG	TCACAACCCAAGAACCAC
FAS	M76767	TGGGCCCAGCTTCTTAGCC	GGAACAGCGCAGTACCGTAGA
PPARα	NM_013196	TGAACAAAGACGGGATG	TCAAACTTGGGTTCCATGAT
CPT-1a	NM_031559	GGTGGGCCACAAATTACGTG	CAGCATCTCCATGGCGTAGT
UCP-2	NM_019354	TCTCCCAATGTTGCCCGAAA	GGGAGGTCGTCTGTCATGAG
Foxa2	NM_012743	TGAAGATGGAAGGGCACGAG	CCCACATAGGATGACATGTTC
ACOX	J02752	ATGGCAGTCCGGAGAATACCC	CCTCATAACGCTGGCTTCGAGT
CYP2E1	NM_031543	AAAGCGTGTGTGTGTTGGAGAA	AGAGACTTCAGGTTAAAATGCTGCA
CYP4A1	NM_175837	TTGAGCTACTGCCAGATCCCAC	CCCATTTTTGGACTTCAGCACA
SCD1	NM_139192	CTCCACTGCTGGACATGAGA	AATGAGTGAAGGGGCACAAC
ATF3	M63282	GAGCGAAGACTGGAGCAAAA	AAGGTGCTTGTTCTGGATGG
XBP1	NM_001004210	TCTCAATCACAAGCCCATGA	GAGCAGCAAGTGGTGGATTT
CHOP	U30186	CCAGCAGAGGTCACAAGCAC	CGCACTGACCACTCTGTTTC
18s rRNA	M11188	GTAACCCGTTGAACCCCATT	CCATCCAATCGGTAGTAGCG

control diet or the HFC diet were measured at the end of the 8-week treatment period. The HFC diet–fed *fa/fa* rats (the HFC rats) showed weight loss (506 ± 26 g, mean ± SEM), in particular, decreasing significantly ($P < .05$) compared with the control diet–fed *fa/fa* rats (the control rats, 571 ± 5.2 g). Similarly, the mean daily food intake of the HFC rats decreased significantly ($P < .05$) compared with the control rats (Table 3), suggesting that reduction of body weights might be associated with fatty diarrhea from the beginning of the feeding in obese *fa/fa* Zucker rats fed with the HFC diet and that the HFC diet might be easy to be induced to the liver. Because the liver weight of the HFC rats was 4-fold higher than that of the control rats (53.2 ± 0.5 vs 13.3 ± 0.5 g, respectively). The weight of the intraabdominal fat was not different between the control and HFC rats. Concentrations of fasting plasma glucose (8.2 ± 0.5 vs 5.6 ± 0.3 mmol/L, $P < .05$), cholesterol (1360 ± 74 vs 128 ± 1.5 mg/dL, $P < .05$), and serum NEFAs (1.77 ± 0.11 vs 1.15 ± 0.19 mEq/L, $P < .05$) were all significantly higher in the HFC rats than in the control rats. However, plasma triglyceride concentrations of the HFC rats were significantly lower than those of the control rats (229 ± 13.6 vs 335 ± 30.3 mg/dL, $P < .05$). Plasma insulin concentrations were not different between the control and HFC rats (17.4 ± 0.9 vs 15.5 ± 0.5 ng/mL).

Table 3
Effects of HFC treatment on metabolic parameters in HFC diet–induced rats with NASH at 8 weeks of treatment

Diet type	Obese (*fa/fa*) Zucker rats	
	Control	HFC
Body weight (g)	571 ± 5.2	506 ± 25.9
Food intake (g/d)	26.3 ± 3.8	21.8 ± 3.8
Liver weight (g)	13.3 ± 0.5	53.2 ± 0.5*
Intraabdominal fat weight (g)	37.3 ± 1.7	34.8 ± 4.2
Epididymal fat pad weight (g)	14.6 ± 0.9	12 ± 0.2
Mesenteric fat weight (g)	7.2 ± 0.4	6.1 ± 0.5
Perinephric fat weight (g)	15.7 ± 1.6	17.2 ± 3.7
Plasma glucose (mmol/L)	5.6 ± 0.3	8.2 ± 0.5*
Plasma insulin (ng/mL)	17.4 ± 0.9	15.5 ± 0.5
Plasma total cholesterol (mg/dL)	128 ± 1.5	1360 ± 74*
Plasma triglycerides (mg/dL)	335 ± 30.3	229 ± 13.6
Serum NEFAs (mEq/L)	1.15 ± 0.19	1.77 ± 0.11*

Values are expressed as mean ± SEM (n = 8).
* $P < .05$ for HFC diet–induced rats vs control diet–induced rats.

3.2. Antioxidant defense activities

Levels of GSH were lowest in the HFC rats (Table 4). The lowest activities of SOD, GPx, and especially CAT were found with the HFC rats (Table 4). The thiobarbituric acid reactive substances (TBARS) levels in the HFC rats

Table 4
Effects of HFC treatment on antioxidant defense enzymes in HFC diet–induced rats with NASH at 8 weeks of treatment

Treatment	GSH	SOD	CAT	GPx
fa/fa control	61 ± 5.5	96 ± 10	5956 ± 278	604 ± 20
fa/fa HFC	42 ± 5*	54 ± 7.1*	1381 ± 141*	356 ± 43*

Values are expressed as mean ± SEM (n = 8). Levels of GSH were measured and expressed as nanomoles per milligram of protein. The activities of total SOD, CAT, and total GPx were measured and expressed as units per milligram of protein.
* $P < .05$ for HFC diet–induced rats vs control diet–induced rats.

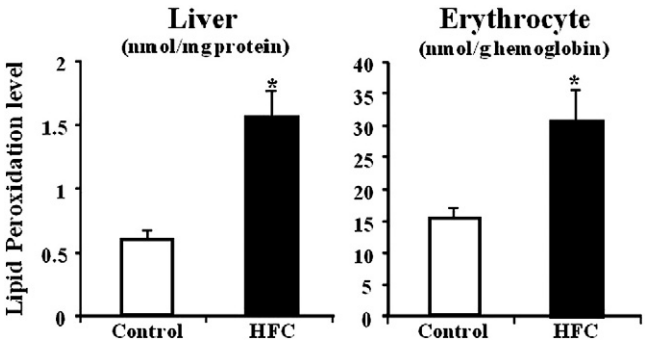

Fig. 1. Comparison of lipid peroxidation levels (TBARS) in the liver and erythrocytes between control diet–induced rats (control) and HFC diet–induced rats (HFC). The TBARS values are indicated as nanomoles per milligram protein in the liver and as nanomoles per gram hemoglobin in erythrocytes. Values are expressed as mean ± SEM (n = 8). *$P < .05$ for HFC diet–induced rats vs control diet–induced rats.

increased significantly ($P < .05$) compared with the control rats (Fig. 1).

3.3. Liver histopathology and the hepatic triglyceride content in the HFC rats

Foci of lobular inflammation appeared scattered in the livers of the HFC rats (Fig. 2A). The HFC rats developed steatohepatitis and ballooning degeneration, and also showed significant macrosteatosis extending beyond the periportal area into the lobule and the central zone (Fig. 2A). Thus, the HFC diet–induced steatosis and inflammation were more severe in the HFC rats at 8 weeks than in the control rats ($P < .05$; Fig. 2A, C). In addition, the HFC diet accelerated the severity of fibrosis, which appeared perisinusoidal/pericellular and as portal fibrosis with focal or extensive bridging fibrosis in the *fa/fa*

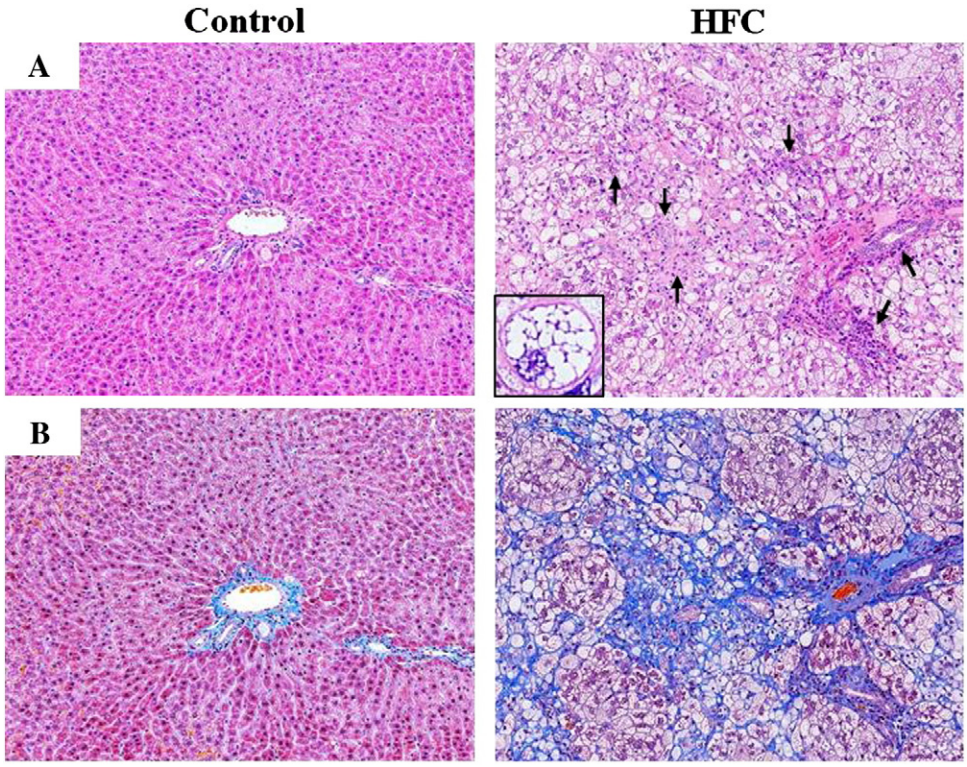

C

Diet type	Obese (*fa/fa*) Zucker rats: Control	HFC
Steatosis (%)	1.8 ± 1.3	88.7 ± 8.1*
Activity (inflammation)	0.4 ± 0.2	5.5 ± 0.5*
Stage (fibrosis)	0	3*
Histological diagnosis	normal	steatohepatitis

Fig. 2. Liver histopathology. Photomicrographs of liver samples stained with hematoxylin and eosin (A) and Mason trichrome (B) after 8 weeks on the control diet or HFC diet. Hepatocyte ballooning is shown in the insets. Arrows indicate infiltration of the inflammatory cells in hepatic parenchyma and portal tract. Original magnification, 100×. Criteria for each score are described in "Materials and methods." Histologic diagnosis at 8 weeks (C). Values are expressed as mean ± SEM (n = 8). *$P < .05$ for HFC diet–induced rats vs control diet–induced rats.

rats (Fig. 2B), and also caused progression of fibrosis in these rats ($P < .05$; Fig. 2B, C).

The HFC rats showed macrovesicular steatosis in the liver (Fig. 2A). Therefore, the hepatic triglyceride content was measured to evaluate the progression of steatosis quantitatively after 8 weeks (Fig. 3A). Hepatic triglyceride content increased significantly in the HFC diet ($P < .05$ vs the control rats). Plasma ALT levels were about 1.9-fold higher in the HFC rats than in the control rats (Fig. 3B). As observed above, the HFC rats met the definitions of NASH.

3.4. Expression of adiponectin, adiponectin receptors (AdipoR1/R2), and insulin receptor substrate (IRS-1/-2)

In the adipose tissue of NASH, the gene expression level of adiponectin was lower than in control rats; however, there were no significant differences between NASH and control rats, respectively (Fig. 4A). The expression levels of the adiponectin receptor (AdipoR1/R2) genes were significantly down-regulated (0.74- and 0.67-fold, respectively) in the liver of NASH compared with control rats (Fig. 4A).

In the liver of NASH, the expression level of IRS-1 was significantly increased 2.8-fold; and IRS-2 was significantly decreased 0.48-fold compared with control rats (Fig. 4A).

3.5. Expression of genes related to de novo synthesis of fatty acids

In the process of fatty acid synthesis, on binding, AdipoR1/R2 activates AMPK, triggering the phosphorylation of ACC; and then ACC converts acetyl-CoA, an essential substrate of fatty acids, to malonyl-CoA [28]. In addition, both ACC and FAS are positively regulated by SREBP-1c [29,30]. In the liver of NASH, the expression levels of genes encoding key regulators of fatty acid synthesis, including ACC, FAS, and SREBP-1c, were significantly up-regulated (5.5-, 4.8-, and 6.8-fold, respectively) compared with control rats (Fig. 4B).

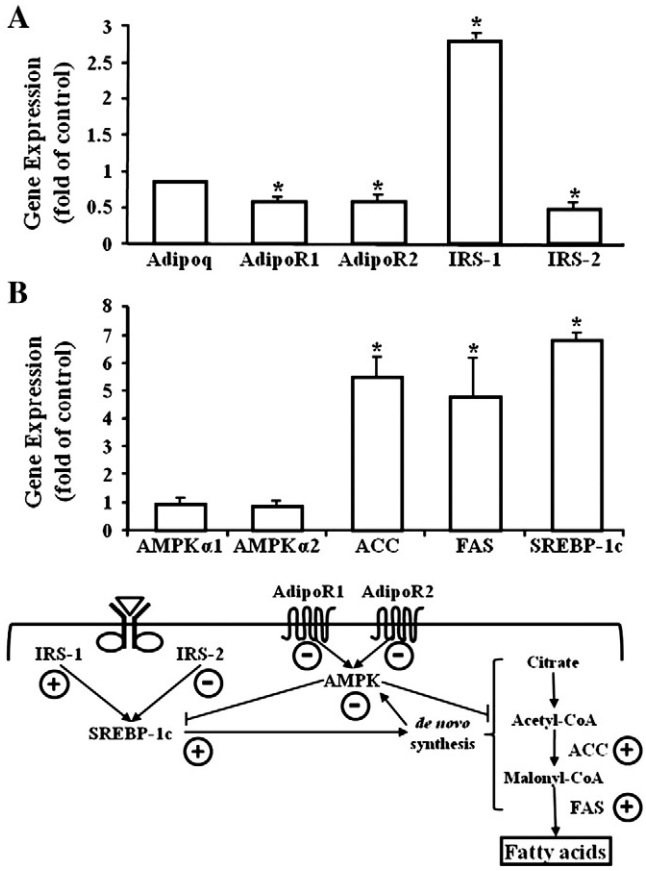

Fig. 4. Real-time PCR analysis for gene expression of adiponectin and AdipoR1/R2 and IRS-1/-2 (A) and de novo synthesis (B) of fatty acids in NASH. Values are expressed as mean ± SEM (n = 8). *$P < .05$ for NASH rats vs control rats. Adipoq indicates adiponectin.

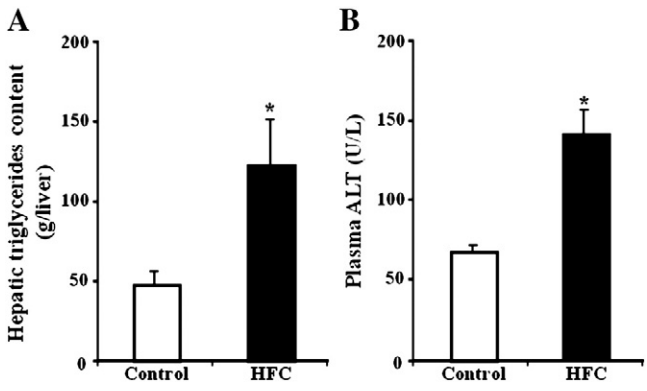

Fig. 3. Hepatic triglyceride content (A) and plasma ALT levels (B) in control diet–induced rats (control) and HFC diet–induced rats (HFC) groups. Hepatic triglyceride content values are indicated as grams per liter in the liver, and plasma ALT values are indicated as units per liter in the plasma. Values are expressed as mean ± SEM (n = 8). *$P < .05$ for HFC diet–induced rats vs control diet–induced rats.

3.6. Gene expression related to fatty acid oxidation in mitochondria, peroxisomes, and microsomes

CPT-1a is a regulatory enzyme in mitochondria that transfers fatty acids from the cytosol to mitochondria before β-oxidation [31]. In the liver of NASH, the messenger RNA (mRNA) expression level of CPT-1a was significantly decreased 0.24-fold compared with control rats (Fig. 5). In the liver of NASH, gene expression level of PPARα was significantly down-regulated (5.4-fold) compared with control rats, whereas the expression levels of UCP-2, ACOX, CYP4A1, and CYP2E1 were significantly up-regulated (3.3-, 3.5-, 12.4-, and 3.6-fold, respectively) compared with control rats (Fig. 5).

Recently, IRSs have been reported to negatively regulate another transcriptional factor, Foxa2, which enhances β-oxidation of fatty acids [14]. In the liver of NASH, the expression level of Foxa2 was 3.0-fold higher than control rats (Fig. 5).

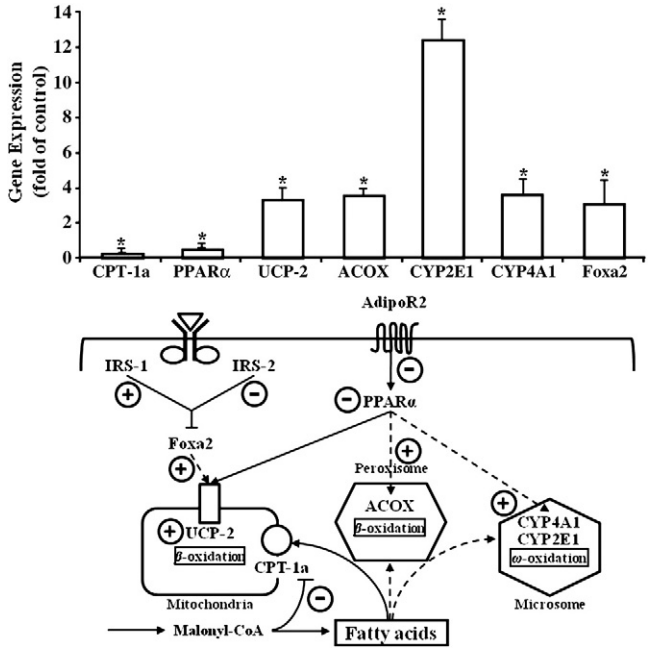

Fig. 5. Real-time PCR analysis for gene expression of oxidation of fatty acids in NASH. Values are expressed as mean ± SEM (n = 8). *$P < .05$ for NASH rats vs control rats.

3.7. Gene expression related to synthesis of monounsaturated fatty acids from saturated fatty acids

Stearoyl-CoA desaturase 1 converts saturated fatty acids to monounsaturated fatty acids, which are major substrates for synthesis of triacylglycerols and other lipids [32]. In the liver of NASH, the expression level of SCD1 was significantly increased 2.3-fold compared with control rats (data not shown).

3.8. Gene expression related to ER stress

Endoplasmic reticulum stress and activation of the unfolded protein response (UPR) in the liver have been observed in dietary models of NAFLD and in humans with NAFLD [33,34]. In the liver of NASH, the expression levels of genes relating to ER stress, including ATF3, XBP1, and CHOP, were significantly up-regulated (3.2-, 2.6-, and 3.0-fold, respectively) compared with control rats (data not shown).

4. Discussion

In the present study, we showed that *fa/fa* rats fed the HFC diet for 8 weeks developed insulin resistance, hyperglycemia, and hyperlipidemia; in addition, the fatty liver spontaneously developed intralobular inflammation with ballooning degeneration, Mallory hyaline bodies, and pericellular fibrosis in the intralobular spaces, which are all characteristics of NASH. The liver inflammation and fibrosis observed in this model could be the result of a "second hit" to NASH, following the known progression of hepatic steatosis [35]. The development of fatty liver into NASH has been linked to oxidative stress and lipid peroxidation in the liver, leading to inflammation [36-38]. We have also shown, for the first time, the dynamic panel of gene expression related to de novo synthesis and oxidation of fatty acids under the controls of AdipoR1/R2 or IRS-1/-2 in the NASH liver.

The liver of NASH showed significantly down-regulated expression of the genes for AdipoR1/R2, although no significant changes were observed in adiponectin gene expression. AdipoR1/R2 expression in humans and mice of NAFLD with obesity, respectively, has been shown to be decreased [39,40]. Plasma adiponectin levels and the expression levels of AdipoR1/R2 have also been shown to be decreased in obesity and insulin resistance [41]. These reports suggested that obesity decreases not only plasma adiponectin levels but also AdipoR1/R2 expression, thereby reducing adiponectin sensitivity and leading to insulin resistance, which in turn aggravates hyperinsulinemia, creating a "vicious cycle" [41]. Thus, AdipoR1/R2 expressions in the liver of NASH with obesity and insulin resistance might be lower than control rats. Bullen et al [42], however, reported that AdipoR1/R2 expression in the liver of high-fat diet–induced mice have been shown to be increased, suggesting that the model used in this study is a model of high-fat diet added on the background of functional leptin deficiency (genetic background of rodents used herein); and this may explain the differences from data reported by Bullen et al. Further studies are necessary to clarify the mechanism of regulation of adiponectin receptors including leptin or leptin resistance in NASH.

Gene expression levels related to *de novo* synthesis of fatty acids in the liver of NASH were significantly up-regulated compared with control rats, whereas those levels of AMPKα1/α2, which were activated by AdipoR1/R2, were down-regulated compared with control rats. In the present study, a positive correlation was found between ACC, FAS, and SREBP-1c expressions. Both ACC and FAS expressions are positively regulated by SREBP-1c [30]. Adenosine monophosphate–activated protein kinase activation inhibits ACC expression indirectly via the suppression of SREBP-1c, and AMPK is activated by adiponectin [28]. Therefore, hypoadiponectinemia might contribute to the down-regulation of the expression of AMPK in the liver of NASH.

Sterol regulatory element binding protein–1c is suppressed by AMPK, whereas it is activated by insulin signaling pathways including IRSs [29,43]. In the present study, IRS-1 expression was significantly elevated and a positive correlation with SREBP-1c expression was observed in the liver of NASH; however, IRS-2 expression was significantly reduced. Recent reports showed that IRS-2 expression, not IRS-1, is down-regulated in the liver of *ob/ob* mice with insulin resistance, whereas SREBP-1c expression is up-regulated [44]. Ide et al [17] reported that the up-regulation of SREBP-1c expression induces hepatic insulin resistance through suppression of IRS-2 expression.

Our study showed that a positive correlation existed between fatty acid de novo synthesis enzymes of ACC, FAS, and SREBP-1c in the liver of NASH. Previous reports and our findings indicated that the up-regulation of SREBP-1c not only increases ACC and FAS expression, but also suppresses IRS-2 expression via a negative feedback mechanism. It is well known that insulin resistance in liver is associated with the down-regulation of both IRS-1/-2 [16,18]. The present study, however, showed the up-regulation of IRS-1 in the liver of NASH, suggesting that the insulin signaling pathways are disrupted there, particularly in terms of normally coordinated regulation between IRS-1 and IRS-2. Generally, IRS-1 is linked more closely to glucose homeostasis and IRS-2 to lipid metabolism [15]. It has been shown that in liver-specific knockout of IRS-1 or IRS-2 expression in C57BL/6 mice, the knockout of hepatic IRS-1 resulted in an up-regulation of gene expression of the gluconeogenic enzymes, whereas knockout of IRS-2 resulted in the up-regulation of lipogenic enzymes of SREBP-1c and FAS, as well as increased hepatic lipid accumulation [15]. Taniguchi et al [15] suggested that hepatic IRS-1/-2 have complementary roles in the control of hepatocyte metabolism; and in the liver of NASH, the up-regulation of IRS-1 may be compensated for by the down-regulation of IRS-2, which was suppressed by SREBP-1c. Our results suggest that when fatty acids synthesis of IRS-2 failed in the liver of NASH, the switch from IRS-2 to IRS-1 can occur; and the up-regulation of SREBP-1c by IRS-1 might result in enhanced fatty acids synthesis. Interestingly, in the liver of high-fat–fed rats, IRS-1 protein level, but not IRS-2, was slightly increased; and insulin-stimulated tyrosine phosphorylation levels of hepatic IRS-1 were higher than controls [19]. Further studies are necessary to clarify the mechanism of up-regulation of hepatic IRS-1 in NASH.

Peroxisome proliferator–activated receptor α up-regulates the expression of a suite of genes that includes mitochondrial, peroxisomal, and microsomal fatty acid oxidation enzymes in liver. However, PPARα expression in the liver of NASH in this current study were significantly down-regulated, whereas mRNA expression of other genes related to oxidation of fatty acids were significantly up-regulated. A recent study reported that the down-regulation of AdipoR2 expression is attributable to decreased PPARα expression in NASH, which agrees with our findings [39]. In this study, we found the down-regulation of AdipoR2 expression in the liver of NASH. Thus, AdipoR2 might be a major regulator of PPARα in the liver of NASH. Uncoupling protein–2 is known to reduce potential ROS production in mitochondria [45]. The up-regulation of UCP-2 found in this study suggested that UCP-2 may increase the mitochondrial β-oxidation of fatty acids in the liver of NASH [46] and that excess ROS production occurs by increased β-oxidation. In addition, in mitochondrial β-oxidation, the mRNA expression level of CPT-1a, an independent enzyme for β-oxidation from PPARα, was down-regulated in the liver of NASH, suggesting that it is attributable to an increase in malonyl-CoA [47] because the expression of ACC, catalyzing acetyl-CoA to malonyl-CoA, was increased.

Excessive fatty acids in hepatocytes activate alternative pathways of fatty acid oxidation, such as β-oxidation occurring by ACOX in peroxisomes and ω-oxidation by CYP2E1/CYP4A1 in microsomes [48]. Thus, the observed elevations of peroxisomal β-oxidation gene expression (ACOX) and of microsomal ω-oxidation (CYP4A1 and CYP2E1) might be due to compensation in the liver of NASH, suggesting that accumulation of fatty acids enhances oxidation not only in mitochondria but also in peroxisomes and microsomes in the liver of NASH. In addition, we found that the enhancement of mRNA expression levels of ACOX and CYP4A1 (3.5- and 3.6-fold, respectively) was less than that of CYP2E1 (12.4-fold), which is not regulated by PPARα. The differences in the expression of oxidation enzymes of ACOX in peroxisomes and CYP4A1 in microsomes might be attributable to the down-regulation of PPARα in the liver of NASH.

Positive fatty acid β-oxidation regulator of Foxa2 is normally suppressed by both IRS-1 and IRS-2 [14]. However, despite a decrease of IRS-2 expression, the observed significant increase of Foxa2 expression in the liver of NASH in comparison might be correlated with the net balance between decreased IRS-2 and increased IRS-1. Taken together with our findings, it is suggested that the up-regulation of Foxa2 was enhanced by suppressed IRS-2 via a negative feedback of SREBP-1c. Thus, IRS-2 could be a major regulator of Foxa2 in the liver with NASH. Recently, it was reported that Foxa2 plays a regulation role in lipid metabolism, such as UCP-2 expression with mitochondrial β-oxidation in the liver, and improves hepatic insulin resistance in diabetic or insulin resistance mice [14]. We showed the up-regulation of UCP-2, suggesting that the up-regulation of Foxa2 and UCP-2 leads to an increase in fatty acid β-oxidation in the liver of NASH.

In conclusion, our NASH animal model indicated various gene expression dynamics and suggested their possible regulatory roles for fatty acids synthesis and oxidation as follows: (1) The mRNA down-regulation of AdipoR1/R2 and AMPKα1/α2 induced fatty acid synthesis through the up-regulation of SREBP-1c, which is stimulated by the up-regulation of IRS-1. (2) The up-regulation of Foxa2 via a negative feedback of the down-regulation of IRS-2, which is suppressed by increased SREBP-1c, induced fatty acid β-oxidation in UCP-2; and mitochondrial fatty acid β-oxidation was increased to improve fatty acid accumulation. (3) Despite the down-regulation of AdipoR2 and PPARα, fatty acid oxidation was increased; and when there is an excess of fatty acids in hepatocytes, alternative pathways of fatty acid oxidation, such as peroxisomal β-oxidation and microsomal ω-oxidation, are increased in compensation. Thus, the present NASH model system can be applied to further studies of the pathology, treatment, and prevention of this recently increasing abnormal liver dysfunction associated with synthesis and oxidation of fatty acids. In addition, we

found that the enhancement of mRNA expression levels of genes related to ER stress. These results suggest that the UPR responds to the fatty acids environment and also indicate that the ratio of saturated fatty acids may be an important determinant of hepatic ER homeostasis. Future studies are necessary to determine whether ER stress and activation of the UPR are causally linked to saturated fatty acid–induced apoptosis and NASH.

Acknowledgment

This study was partially supported by the Academic Frontier Project "Surveillance and control for zoonoses" and the Strategic Research Base Development Program "International research on epidemiology of zoonoses and training for young researchers" from the Ministry of Education, Culture, Sports, Science, and Technology, Japan.

References

[1] Ludwig J, McGill DB, Lindor KD. Review: nonalcoholic steatohepatitis. J Gastroenterol Hepatol 1997;12:398-403.
[2] McCullough AJ. Update on nonalcoholic fatty liver disease. J Clin Gastroenterol 2002;34:255-62.
[3] Fruebis J, Tsao TS, Javorschi S, et al. Proteolytic cleavage product of 30-kDa adipocyte complement-related protein increases fatty acid oxidation in muscle and causes weight loss in mice. Proc Natl Acad Sci U S A 2001;98:2005-10.
[4] Yamauchi T, Kamon J, Minokoshi Y, et al. Adiponectin stimulates glucose utilization and fatty-acid oxidation by activating AMP-activated protein kinase. Nat Med 2002;8:1288-95.
[5] Yamauchi T, Nio Y, Maki T, et al. Targeted disruption of AdipoR1 and AdipoR2 causes abrogation of adiponectin binding and metabolic actions. Nat Med 2007;13:332-9.
[6] Kadowaki T, Yamauchi T. Adiponectin and adiponectin receptors. Endocr Rev 2005;26:439-51.
[7] Musso G, Gambino R, De Michieli F, et al. Nitrosative stress predicts the presence and severity of nonalcoholic fatty liver at different stages of the development of insulin resistance and metabolic syndrome: possible role of vitamin A intake. Am J Clin Nutr 2007;86:661-71.
[8] Tsochatzis E, Papatheodoridis GV, Archimandritis AJ. The evolving role of leptin and adiponectin in chronic liver diseases. Am J Gastroenterol 2006;101:2629-40.
[9] Kaser S, Moschen A, Cayon A, et al. Adiponectin and its receptors in non-alcoholic steatohepatitis. Gut 2005;54:117-21.
[10] Vuppalanchi R, Marri S, Kolwankar D, et al. Is adiponectin involved in the pathogenesis of nonalcoholic steatohepatitis? A preliminary human study. J Clin Gastroenterol 2005;39:237-42.
[11] Osborne TF. Sterol regulatory element-binding proteins (SREBPs): key regulators of nutritional homeostasis and insulin action. J Biol Chem 2000;275:32379-82.
[12] Matsuzaka T, Shimano H, Yahagi N, et al. Insulin-independent induction of sterol regulatory element-binding protein–1c expression in the livers of streptozotocin-treated mice. Diabetes 2004;53:560-9.
[13] Kerouz NJ, Horsch D, Pons S, Kahn CR. Differential regulation of insulin receptor substrates–1 and –2 (IRS-1 and IRS-2) and phosphatidylinositol 3-kinase isoforms in liver and muscle of the obese diabetic (*ob/ob*) mouse. J Clin Invest 1997;100:3164-72.
[14] Wolfrum C, Asilmaz E, Luca E, Friedman JM, Stoffel M. Foxa2 regulates lipid metabolism and ketogenesis in the liver during fasting and in diabetes. Nature 2004;432:1027-32.
[15] Taniguchi CM, Ueki K, Kahn R. Complementary roles of IRS-1 and IRS-2 in the hepatic regulation of metabolism. J Clin Invest 2005;115:718-27.
[16] Valverde AM, Arribas M, Mur C, et al. Insulin-induced up-regulated uncoupling protein–1 expression is mediated by insulin receptor substrate 1 through the phosphatidylinositol 3-kinase/Akt signaling pathway in fetal brown adipocytes. J Biol Chem 2003;278:10221-31.
[17] Ide T, Shimano H, Yahagi N, et al. SREBPs suppress IRS-2–mediated insulin signalling in the liver. Nat Cell Biol 2004;6:351-7.
[18] Dong X, Park S, Lin X, et al. Irs1 and Irs2 signaling is essential for hepatic glucose homeostasis and systemic growth. J Clin Invest 2006;116:101-14.
[19] Anai M, Funaki M, Ogihara T, et al. Enhanced insulin-stimulated activation of phosphatidylinositol 3-kinase in the liver of high-fat–fed rats. Diabetes 1999;48:158-69.
[20] Meister A. Glutathione deficiency produced by inhibition of its synthesis, and its reversal; applications in research and therapy. Pharmacol Ther 1991;51:155-94.
[21] Sun Y, Oberley LW, Li Y. A simple method for clinical assay of superoxide dismutase. Clin Chem 1988;34:497-500.
[22] Aebi H. Catalase in vitro. Methods Enzymol 1984;105:121-6.
[23] Paglia DE, Valentine WN. Studies on the quantitative and qualitative characterization of erythrocyte glutathione peroxidase. J Lab Clin Med 1967;70:158-69.
[24] Ohkawa H, Ohishi N, Yagi K. Assay for lipid peroxides in animal tissues by thiobarbituric acid reaction. Anal Biochem 1979;95:351-8.
[25] Brunt EM, Janney CG, Di Bisceglie AM, et al. Nonalcoholic steatohepatitis: a proposal for grading and staging the histological lesions. Am J Gastroenterol 1999;94:2467-74.
[26] Schmittgen TD, Zakrajsek BA. Effect of experimental treatment on housekeeping gene expression: validation by real-time, quantitative RT-PCR. J Biochem Biophys Methods 2000;46:69-81.
[27] Pfaffl MW. A new mathematical model for relative quantification in real-time RT-PCR. Nucleic Acids Res 2001;29:e45.
[28] Long YC, Zierath JR. AMP-activated protein kinase signaling in metabolic regulation. J Clin Invest 2006;116:1776-83.
[29] Zhou G, Myers R, Li Y, et al. Role of AMP-activated protein kinase in mechanism of metformin action. J Clin Invest 2001;108:1167-74.
[30] Leff T. AMP-activated protein kinase regulates gene expression by direct phosphorylation of nuclear proteins. Biochem Soc Trans 2003;31:224-7.
[31] Rodriguez MI, Escames G, Lopez LC, et al. Improved mitochondrial function and increased life span after chronic melatonin treatment in senescent prone mice. Exp Gerontol 2008;43:749-56.
[32] Ntambi JM, Miyazaki M. Regulation of stearoyl-CoA desaturases and role in metabolism. Prog Lipid Res 2004;43:91-104.
[33] Wang CH, Leung CH, Liu SC, et al. Safety and effectiveness of rosiglitazone in type 2 diabetes patients with nonalcoholic fatty liver disease. J Formos Med Assoc 2006;105:743-52.
[34] Puri P, Mirshahi F, Cheung O, et al. Activation and dysregulation of the unfolded protein response in nonalcoholic fatty liver disease. Gastroenterology 2008;134:568-76.
[35] Day CP. Pathogenesis of steatohepatitis. Best Pract Res Clin 2002;16:663-78.
[36] George J. Ascorbic acid concentrations in dimethylnitrosamine-induced hepatic fibrosis in rats. Clin Chim Acta 2003;335:39-47.
[37] Browning JD, Horton JD. Molecular mediators of hepatic steatosis and liver injury. J Clin Invest 2004;114:147-52.
[38] Carmiel-Haggai M, Cederbaum AI, Nieto N. A high-fat diet leads to the progression of non-alcoholic fatty liver disease in obese rats. FASEB J 2005;19:136-8.
[39] Tomita K, Oike Y, Teratani T, et al. Hepatic AdipoR2 signaling plays a protective role against progression of nonalcoholic steatohepatitis in mice. Hepatology 2008;48:458-73.
[40] Ma H, Gomez V, Lu L, et al. Expression of adiponectin and its receptors in livers of morbidly obese patients with non-alcoholic fatty liver disease. J Gastroenterol Hepatol 2009;24:233-7.

[41] Tsuchida A, Yamauchi T, Ito Y, et al. Insulin/Foxo1 pathway regulates expression levels of adiponectin receptors and adiponectin sensitivity. J Biol Chem 2004;279:30817-22.

[42] Bullen Jr JW, Bluher S, Kelesidis T, et al. Regulation of adiponectin and its receptors in response to development of diet-induced obesity in mice. Am J Physiol Endocrinol Metab 2007;292: E1079-E1086.

[43] Woods A, Azzout-Marniche D, Foretz M, et al. Characterization of the role of AMP-activated protein kinase in the regulation of glucose-activated gene expression using constitutively active and dominant negative forms of the kinase. Mol Cell Biol 2000;20:6704-11.

[44] Shimomura I, Matsuda M, Hammer RE, et al. Decreased IRS-2 and increased SREBP-1c lead to mixed insulin resistance and sensitivity in livers of lipodystrophic and *ob/ob* mice. Mol Cell 2000;6:77-86.

[45] Pessayre D, Berson A, Fromenty B, et al. Mitochondria in steatohepatitis. Semin Liver Dis 2001;21:57-69.

[46] Miele L, Grieco A, Armuzzi A, et al. Hepatic mitochondrial beta-oxidation in patients with nonalcoholic steatohepatitis assessed by 13C-octanoate breath test. Am J Gastroenterol 2003;98:2335-6.

[47] Grum DE, Hansen LR, Drackley JK. Peroxisomal beta-oxidation of fatty acids in bovine and rat liver. Comp Biochem Physiol 1994;109: 281-92.

[48] Reddy JK, Hashimoto T. Peroxisomal beta-oxidation and peroxisome proliferator-activated receptor alpha: an adaptive metabolic system. Annu Rev Nutr 2001;21:193-230.